



Published in final edited form as:

*Circulation*. 2014 April 22; 129(16): 1677–1687. doi:10.1161/CIRCULATIONAHA.113.006381.

## Innate Response Activator B Cells Aggravate Atherosclerosis by Stimulating T<sub>H1</sub> Adaptive Immunity

Ingo Hilgendorf, MD<sup>1,\*</sup>, Igor Theurl, MD, PhD<sup>1,2,\*</sup>, Louisa M.S. Gerhardt, MS<sup>1</sup>, Clinton S. Robbins, PhD<sup>1,3</sup>, Georg F. Weber, MD<sup>1</sup>, Ayelet Gonen, PhD<sup>4</sup>, Yoshiko Iwamoto, BS<sup>1</sup>, Norbert Degousee, PhD<sup>2</sup>, Tobias A. W. Holderried, MD<sup>5</sup>, Carla Winter, BS<sup>1,6</sup>, Andreas Zirlik, MD<sup>6</sup>, Herbert Y. Lin, MD<sup>1</sup>, Galina K. Sukhova, PhD<sup>7</sup>, Jagdish Butany, MD<sup>8</sup>, Barry B. Rubin, MD, PhD<sup>9</sup>, Joseph L. Witztum, PhD<sup>4</sup>, Peter Libby, MD<sup>7</sup>, Matthias Nahrendorf, MD, PhD<sup>1</sup>, Ralph Weissleder, MD, PhD<sup>1,10</sup>, and Filip K. Swirski, PhD<sup>1</sup>

<sup>1</sup>Center for Systems Biology, Massachusetts General Hospital, Boston, MA

<sup>2</sup>Department of Internal Medicine IV, Infectious Diseases, Immunology Rheumatology, Pneumology, University Hospital of Innsbruck, Innsbruck, Austria

<sup>3</sup>Toronto General Research Institute, University Health Network, Toronto, ON, Canada

<sup>4</sup>Department of Medicine, UCSD, La Jolla, CA

<sup>5</sup>Department of Gastroenterology, Hepatology and Infectious Diseases, University of Duesseldorf, Duesseldorf, Germany

<sup>6</sup>Department of Cardiology and Angiology I, University Heart Center Freiburg, Freiburg, Germany

<sup>7</sup>Cardiovascular Division, Department of Medicine, Brigham and Women's Hospital, Boston, MA

<sup>8</sup>Department of Pathology, Peter Munk Cardiac Centre, Toronto General Hospital, Toronto, ON, Canada

<sup>9</sup>Division of Vascular Surgery, Peter Munk Cardiac Centre, Toronto General Hospital, Toronto, ON, Canada

<sup>10</sup>Department of Systems Biology, Harvard Medical School, Boston, MA

### Abstract

**Background**—Atherosclerotic lesions grow via the accumulation of leukocytes and oxidized lipoproteins in the vessel wall. Leukocytes can attenuate or augment atherosclerosis through the release of cytokines, chemokines, and other mediators. Deciphering how leukocytes develop, oppose and complement each other's function, and shape the course of disease, can illuminate understanding of atherosclerosis. Innate response activator (IRA) B cells are a recently described population of GM-CSF-secreting cells of hitherto unknown function in atherosclerosis.

**Correspondence:** Ingo Hilgendorf, MD or Filip K. Swirski, PhD, Center for Systems Biology, Massachusetts General Hospital and Harvard Medical School, Simches Research Building, 185 Cambridge St., Boston, MA 02114, Phone: 617-724-6242, Fax: 617-726-5708, fswirski@mgh.harvard.edu or hilgendorf.ingo@mgh.harvard.edu.

\*contributed equally

**Conflict of Interest Disclosures:** None.

**Methods and Results**—Here we show that IRA B cells arise during atherosclerosis in mice and humans. In response to high cholesterol diet, IRA B cell numbers increase preferentially in secondary lymphoid organs via Myd88-dependent signaling. Mixed chimeric mice lacking B cell-derived GM-CSF develop smaller lesions with fewer macrophages and effector T cells.

Mechanistically, IRA B cells promote the expansion of classical dendritic cells, which then generate IFN $\gamma$ -producing T<sub>H1</sub> cells. This IRA B cell-dependent T<sub>H1</sub> skewing manifests in an IgG1 to IgG2c isotype switch in the immunoglobulin response against oxidized lipoproteins.

**Conclusions**—GM-CSF-producing IRA B cells alter adaptive immune processes and shift the leukocyte response toward a T<sub>H1</sub>-associated milieu that aggravates atherosclerosis.

### Keywords

atherosclerosis; immunology; B cells; Dendritic cells; T cells; Granulocyte macrophage colony-stimulating factor

---

Atherosclerosis is a lipid-driven inflammatory disease that mobilizes a diverse repertoire of leukocytes. Although macrophages accumulate in lesions in greatest number, other leukocytes can modulate the course of disease. Over the last twenty years, many studies have explored how leukocytes influence atherosclerosis. For example, M1 macrophages, T helper-1 (T<sub>H1</sub>) cells, and B2 B cells accelerate, whereas T regulatory (T<sub>reg</sub>) cells and B1 B cells attenuate lesion growth, either by augmenting or restraining inflammation<sup>1-10</sup>. These observations have clinical implications because they suggest that harnessing protective leukocyte activities and silencing those that are harmful could furnish novel treatments for atherosclerosis and other inflammatory diseases.

Innate response activator (IRA) B cells develop in the spleen during the inflammatory phase of sepsis<sup>11</sup>. IRA B cells produce GM-CSF, a pleiotropic growth factor that, although dispensable to hematopoiesis in the steady state, promotes the survival, proliferation, and activity of various leukocytes expressing its receptor<sup>12-14</sup>. The function and source of GM-CSF in atherosclerosis remains obscure. Even though some have reported that GM-CSF protects against atherosclerosis<sup>15</sup>, the weight of evidence suggests that GM-CSF is atherogenic because *Ldlr*<sup>-/-</sup> *Csf2*<sup>-/-</sup> mice develop smaller lesions<sup>16</sup>, whereas exogenous administration of GM-CSF to atherosclerotic mice increases plaque burden<sup>17</sup> and stimulates intimal cell proliferation<sup>18</sup>. In *Apoe*<sup>-/-</sup> mice, hematopoietic stem and progenitor cells (HSPC) elevate expression of the common beta chain ( $\beta_c$ ) of the GM-CSF receptor downstream of impaired reverse cholesterol transport, leading to proliferation that generates leukocytosis and monocytosis<sup>19</sup>. GM-CSF can arise from macrophages, T cells, and epithelial cells, but it remains unknown whether IRA B cells develop in atherosclerosis and, if so, whether they have functional relevance.

### Methods

A detailed description of the methods is available in the online-only Data Supplement.

## Animals

C57Bl/6J (WT), B6.SJL-PtprcaPepcb/BoyJ (CD45.1<sup>+</sup>), B6.129P2(SJL)-Myd88tm1.1Defr/J (Myd88<sup>-/-</sup>), B10.129S2(B6)-Ighmtm1Cgn/J (μMT), B6.Cg-Tg(TcraTcrb)425Cbn/J (OT-II), B6.129S7-Ldlrtm1Her/J (Ldlr<sup>-/-</sup>) and B6.129P2-Apoetm1Unc/J (ApoE<sup>-/-</sup>) were purchased from The Jackson Laboratory (Bar Harbor, ME). GM-CSF-deficient mice (Csf2<sup>-/-</sup>) were kindly provided by Dr. Randy Seeley, University of Cincinnati, USA. GM-CSF-receptor deficient mice (Csf2rb<sup>-/-</sup>) were kindly provided by Dr. Jeffrey Whitsett, Cincinnati Children's Hospital Medical Center, USA. All protocols are approved by the Animal Review Committee at Massachusetts General Hospital.

## Animal experiments

Mixed bone marrow chimeras were generated by lethally irradiating 8 weeks old male Ldlr<sup>-/-</sup> mice and reconstituting with a 50:50 mixture of Csf2<sup>-/-</sup> with WT (Controls) and μMT bone marrow cells (IRA B KO), or with CD45.1<sup>+</sup>, Myd88<sup>-/-</sup> and Csf2rb<sup>-/-</sup> bone marrow. For adoptive transfer studies 25 × 10<sup>6</sup> CD19<sup>+</sup> B cells from WT and Csf2<sup>-/-</sup> mice, respectively, were injected intravenously twice per mouse, 4 weeks apart.

## Histology

Murine aortas and spleens were embedded in Tissue-Tek O.C.T compound (Sakura Finetek) for sectioning and staining. Human spleen samples were fixed in 10% formalin and embedded in paraffin for histologic sectioning and staining.

## Flow Cytometry

Antibodies used for flow cytometry are listed in the online-only Data Supplement. Data were acquired on a BD LSRII and analyzed with FlowJo.

## Reverse transcription PCR

RNA was isolated from sorted cells with the RNeasy Micro Kit (Qiagen) and from snap-frozen aortas and spleens with the RNeasy Mini Kit (Qiagen). Quantitative real-time TaqMan PCR was run on a 7500 PCR thermal cycler (Applied Biosystems).

## Cell culture

Lineage-depleted bone marrow cells were co-cultured with equal numbers of IRA B cells and murine IL-4 (5000 U/ml) to generate dendritic cells. 1 × 10<sup>4</sup> IRA B cell generated bone marrow derived DC (BMDC) were loaded with 100 μg/ml ovalbumin (OVA) or BSA and co-cultured with 5 × 10<sup>4</sup> labelled OT-II T cells over 4 days for flow cytometric assessment of proliferation. CD4<sup>+</sup> CD25<sup>+</sup> T<sub>reg</sub> cells were sorted from IRA B KO and control mice and co-cultured with sorted CD45.1<sup>+</sup> CD4<sup>+</sup> CD25<sup>-</sup> T<sub>conv</sub> cells at increasing dilutions on T cell-depleted and irradiated splenocytes loaded with 1 μg/ml anti-CD3e. Suppression of T cell proliferation was assessed by flow cytometry after 3 days.

## Statistics

Results are shown as mean ± SEM. The unpaired Student's t test was applied to evaluate differences between two study groups. One-way ANOVA with post-hoc Dunnett's multiple

comparisons test was performed when comparing more than two groups. P-values of 0.05 and less denote significant changes.

## Results

### GM-CSF-producing IRA B cells expand in atherosclerosis

We asked whether IRA B cells develop in atherosclerosis. The spleens of both *Ldlr*<sup>-/-</sup> and *Apoe*<sup>-/-</sup> mice consuming a diet high in fat and cholesterol (HCD) contained a population of GM-CSF-producing cells. Most of these were IgM<sup>high</sup> B220<sup>+</sup> CD23<sup>low</sup> CD21<sup>low</sup> CD138<sup>high</sup> CD43<sup>high</sup> VLA4<sup>high</sup> IRA B cells, resembling IRA B cells generated by LPS stimulation (Figure 1A, Supplemental Figure 1A), as originally described<sup>11</sup>. Immunofluorescence (IF) staining for GM-CSF revealed a population of GM-CSF-producing IgM<sup>+</sup> B cells in the marginal zone and red pulp of the spleen (Figure 1B), a location where IRA B cells typically reside. Analysis of various organs showed preferential IRA B cell accumulation in the spleen, although the bone marrow and lymph nodes also harbored smaller IRA B cell populations (Figure 1C). IRA B cell numbers rose most dramatically and progressively in *Apoe*<sup>-/-</sup> mice (Figure 1D), a finding that agrees with the prevailing notion that *Apoe*<sup>-/-</sup> mice display more severe inflammation and atherosclerosis than *Ldlr*<sup>-/-</sup> mice. B cells accumulate in the aortic adventitia<sup>20</sup>, but we did not detect IRA B cells in the aorta, indicating that IRA B cells do not furnish lesional GM-CSF<sup>21</sup>, and suggesting that IRA B cells do not affect lesions locally. Humans with severe coronary and peripheral artery disease contained more GM-CSF<sup>+</sup> IgM<sup>+</sup> IRA B cells in the spleen compared to humans without atherosclerotic disease (Figure 1E, Supplemental Figure 1B, C). Thus, IRA B cells accumulate in secondary lymphoid organs in humans and mice with atherosclerosis. Future studies will need to determine the exact triggers and risk factors responsible for IRA B cell production.

During experimental sepsis, IRA B cells arise by engaging Myd88-dependent Toll-like-receptors (TLR)<sup>11</sup>. To test whether IRA B cells require Myd88 in atherosclerosis, we generated mixed chimeras by lethally irradiating *Ldlr*<sup>-/-</sup> mice and reconstituting with a mixture of wild type (WT) CD45.1<sup>+</sup> and *Myd88*<sup>-/-</sup> CD45.2<sup>+</sup> bone marrow cells (Supplemental Figure 1D). After reconstitution, mice consumed HCD for 12 weeks. CD45.1<sup>+</sup> WT, but not CD45.2<sup>+</sup> *Myd88*<sup>-/-</sup> cells, developed into IRA B cells, indicating a requirement for direct Myd88 engagement in B cells (Supplemental Figure 1E).

### IRA B cells aggravate atherosclerosis

Determining the impact of IRA B cells on atherosclerosis required selective depletion of GM-CSF from B cells. To achieve this, we adapted the mixed chimeric strategy (Figure 2A). *Ldlr*<sup>-/-</sup> mice were lethally irradiated and reconstituted with a mixture of bone marrow cells from *Csf2*<sup>-/-</sup> (i.e., GM-CSF<sup>-/-</sup>) and  $\mu$ MT mice (i.e., B cell-deficient). In the reconstituted animals, B cells were the only population completely lacking the capacity to produce GM-CSF because only *Csf2*<sup>-/-</sup> cells could give rise to B cells. As controls, we reconstituted *Ldlr*<sup>-/-</sup> mice with bone marrow from *Csf2*<sup>-/-</sup> and WT mice, thus ensuring that differences between the groups – should any arise – would exclusively reflect B cell-derived GM-CSF deficiency while preserving GM-CSF production by other sources. RT-PCR analysis on

sorted B cells, T cells, and myeloid cells confirmed the selective deletion of GM-CSF from B cells (Figure 2B). After 6 weeks of reconstitution, we profiled the leukocyte repertoires in the *Csf2*<sup>-/-</sup>/μMT (henceforth simply referred to as “IRA B KO mice”) and the *Csf2*<sup>-/-</sup>/WT (control) mice. The blood, spleen, bone marrow and peritoneal cavity contained similar numbers of leukocyte subsets in both groups (Supplemental Figure 2A–D), indicating successful reconstitution and a similar leukocyte basal population before the triggering of disease.

After reconstitution, the animals consumed HCD for 10 weeks. GM-CSF expression in the spleen of IRA B KO mice was reduced by 70%, which shows a dominant role for IRA B cells as a source of GM-CSF in the spleen during atherosclerosis (Supplemental Fig 2E). GM-CSF production by other leukocytes was similar between the groups (Supplemental Fig 2F), as were body weights and plasma cholesterol levels (Supplemental Fig 3A). The absence of IRA B cells, however, yielded smaller atherosclerotic lesions in the aorta and in particular the aortic root (Figure 2C, D), diminished lipid- and macrophage-rich areas, and reduced numbers of CD4 T cells, but did not change the smooth muscle cell and collagen content. The changes in lesion size and macrophage content did not depend on circulating monocyte and neutrophil number (Supplemental Figure 3B), as might be expected<sup>9, 14</sup>. Moreover, blood Ly-6C<sup>high</sup> monocytes expressed similar levels of CCR2, VLA4, and CD62L (Supplemental Figure 3C), which argued against a defect in monocytes’ capacity to accumulate.

### IRA B cells promote the expansion of T<sub>H1</sub> effector cells

Numerous studies have identified a role for CD4 T cells in atherosclerosis. Naive CD4 T cells can differentiate into various helper subsets exhibiting either protective or atherogenic properties<sup>1–4, 7, 10, 22</sup>. The observation that lesions in IRA B KO mice accumulated fewer CD4 T cells prompted us to investigate this leukocyte population in more detail. The blood of IRA B KO mice contained both effector CD44<sup>high</sup> CD62L<sup>low</sup> CD4 T cells and regulatory Foxp3<sup>+</sup> T<sub>reg</sub> T cells (Figure 3A). At the onset of the experiment, both groups contained equal numbers of these subsets in the blood and spleen (Figure 3B), but after 10 weeks of HCD IRA B KO mice developed fewer effector T cells in the blood, spleen, and para-aortic lymph nodes compared to controls. T<sub>reg</sub> cells, on the other hand, developed similarly in both groups in terms of number and suppressive function (Figure 3B, Supplemental Figure 4A, B).

Among effector T cells, IFNγ-producing T<sub>H1</sub> cells augment atherosclerosis<sup>2, 10, 22, 23</sup>. We detected fewer IFNγ-producing T<sub>H1</sub> cells in blood, spleen, and lymph nodes in IRA B KO mice compared to controls after 10 week HCD feeding (Figure 3C, D). Neither group differed in the number of splenic T<sub>H17</sub> or IL-4-producing T<sub>H2</sub> cells (Supplemental Figure 4C). Do IRA B cells shape an antigen-specific T<sub>H1</sub> milieu? In atherosclerosis, it is thought that low-density lipoproteins (LDL) generate an adaptive immune response, presumably due to a break in peripheral tolerance against self antigens<sup>24</sup>. LDL also undergoes oxidation, which can mobilize T<sub>H1</sub> responses via antigen presentation in the context of oxidative stress-related danger signals<sup>25, 26</sup>. T<sub>H1</sub> cells contribute to isotype switching, and thus influence antigen-specific humoral immunity<sup>27–29</sup>. T cell-derived IFNγ, for example, induces IgG2a/c

and dampens IgG1 production, whereas IL-4 has the opposite effect<sup>30</sup>. In these experiments, IRA B KO mice were impaired in generating T<sub>H1</sub>-dependent IgG2c antibodies against copper (Cu)-oxidized and MDA-modified LDL, even though total IgG and IgM levels increased similarly in both groups (Figure 3E–G and Supplemental Figure 4D–G). Titers of the atheroprotective IgM natural antibody E06 against oxidation-specific epitopes remained unaffected (Supplemental Figure 3C). Hence, as IRA B cell number rose in secondary lymphoid organs, so did the number of effector IFN $\gamma$ -producing T<sub>H1</sub> cells and concentration of antigen-specific, IFN $\gamma$ -dependent IgG2c. That said, we reasoned that IRA B cells did not augment T cell numbers directly because T cells do not express the GM-CSF receptor<sup>31</sup>.

### IRA B cells promote the generation of classical dendritic cells

Effector T cells arise in lymphoid organs when their T cell receptor (TCR) recognizes antigen on DC. In the context of specific secondary signals, antigen presented on MHCII can give rise to effector T<sub>H1</sub> cells that expand, enter the circulation and tissue, and participate in immunity<sup>32</sup>. Unlike T cells, DC and their precursors express the GM-CSF receptor, and might therefore be directly influenced by IRA B cells. To test this hypothesis, we enumerated DC in the spleen, where IRA B cells expand most prominently. Three populations of CD11c<sup>+</sup> MHCII<sup>+</sup> classical (c)DC were identifiable: CD11b<sup>+</sup> CD8<sup>-</sup> CD103<sup>-</sup>, CD11b<sup>-</sup> CD8<sup>+</sup> CD103<sup>-</sup>, and CD11b<sup>-</sup> CD8<sup>+</sup> CD103<sup>+</sup> (Figure 4A). Before the onset of atherosclerosis, both mouse groups contained similar numbers of all three subsets, in agreement with the observation that GM-CSF does not affect the generation of splenic DC in the steady state<sup>33, 34</sup>. During inflammation and with increased GM-CSF, DC expand<sup>33, 35</sup>. Consequently, over the course of HCD consumption, control mice selectively increased the number of CD11b<sup>+</sup> cDC (Figure 4B). In contrast, IRA B KO mice maintained their cDC numbers at steady state levels in the spleen (Figure 4B) and lymph nodes (Figure 4C). Remarkably, not only did IRA B KO mice generate fewer cDC, but these cDC also expressed less T<sub>H1</sub>-priming IL-12p40 (Figure 4D). Although there were no differences in CD86 and CD40 expression, MHCII decreased slightly on CD11b<sup>+</sup> cDC in IRA B KO mice (Supplemental Figure 5A). IRA B cell deficiency neither affected the generation of GMP and CDP in the bone marrow, nor the number of preDC in the bone marrow and spleen, which argues against an IRA B cell-dependent mobilization and expansion of DC progenitors (Supplemental Figure 5B).

To determine whether the changes in cDC subset and function depended on the direct interaction of GM-CSF with cDC, we reconstituted lethally irradiated *Ldlr*<sup>-/-</sup> mice with a 50:50 mixture of bone marrow cells from CD45.1<sup>+</sup> WT mice and CD45.2<sup>+</sup> mice deficient in the common beta chain of the GM-CSF-receptor (*Csf2rb*<sup>-/-</sup>), and placed them on HCD for 3 months (Figure 4E). Whereas the CD45.1/CD45.2 splenic cDC chimerism was ~50:50 among the CD8<sup>+</sup> subset, chimerism was skewed towards the CD45.1<sup>+</sup> WT cells (60:40) among CD11b<sup>+</sup> cDC, suggesting that *Csf2rb*<sup>-/-</sup> cells were impaired in generating CD11b<sup>+</sup> cDC (Figure 4F). This observation agrees with an earlier report that exogenous GM-CSF administration augmented the number of CD11b<sup>+</sup> but not CD8<sup>+</sup> cDC in the spleen<sup>36</sup>. Moreover, IL-12p40 expression was lower in sorted *Csf2rb*<sup>-/-</sup> cDC compared to WT cDC (Figure 4G), thereby reproducing the main effects we observed in IRA B KO mice and suggesting that IRA B cells influence cDC directly via GM-CSF.



Since dendritic cells can differentiate from bone marrow precursors through culture with recombinant (r)GM-CSF and IL-4, we wondered whether IRA B cells can act as GM-CSF sources capable of generating functionally active DC. We sorted IRA B cells from LPS stimulated WT mice (Figure 4H) and placed them in culture with lineage-depleted (i.e., enriched for HSPC) bone marrow cells and IL-4 (Figure 4I). After 8 days, MHCII<sup>+</sup> CD11c<sup>+</sup> CD40<sup>+</sup> CD86<sup>+</sup> DC appeared (Figure 4J). As controls, we cultured bone marrow cells with IL-4 alone or with B cells from *Csf2*<sup>-/-</sup> mice plus IL-4, and enumerated fewer DC (Figure 4K). The group cultured with IRA B cells yielded more cells with characteristic dendritic cell morphology (Figure 4L), thus complementing the surface marker characteristics. To determine the functionality of IRA B cell-generated DC, we pulsed them with ovalbumin (OVA) and co-cultured with OVA-specific transgenic OT-II CD4<sup>+</sup> cells that had been labeled with a tracer. In the absence of OVA, OT-II cells did not proliferate but, when OVA was added, T cells proliferated robustly, as determined by the progressive loss of their tracer dye (Figure 4M). Likewise, IRA B cells sorted from spleens of atherosclerotic *Ldlr*<sup>-/-</sup> mice generated functional bone marrow-derived DC capable of processing ovalbumin for effective antigen presentation and OT-II cell proliferation (Supplemental Figure 5C, D). These experiments indicate that IRA B cells indeed stimulate the generation of mature DC, which can promote antigen-specific T cell expansion.

### Transfer of GM-CSF-competent B cells aggravates atherosclerosis

If lesions are smaller in the absence of IRA B cells, could the adoptive transfer of GM-CSF-competent B cells into IRA B KO mice give rise to IRA B cells and reverse the phenotype by promoting IFN $\gamma$ -producing T<sub>H1</sub> cells and atherogenesis? To test this conjecture, we adoptively transferred WT B cells (i.e., B cell capable of producing GM-CSF) and *Csf2*<sup>-/-</sup> B cells into IRA B KO mice on HCD, twice, 4 weeks apart (Figure 5A). To establish whether IRA B cells develop in recipient animals, we transferred CD45.1<sup>+</sup> WT B cells into CD45.2<sup>+</sup> IRA B KO mice and profiled their phenotype after 8 weeks of HCD. Remarkably, a population of CD45.1<sup>+</sup> GM-CSF<sup>+</sup> IRA B cells appeared in the spleen (Figure 5B), thus allowing us to determine the impact of IRA B cell delivery on the development of atherosclerosis. The transfer of WT but not *Csf2*<sup>-/-</sup> B cells increased GM-CSF production in the spleen by over 50% and gave rise to a larger number of splenic cDC and blood effector T cells, including IFN $\gamma$ -producing T<sub>H1</sub> cells (Figure 5C, D). Moreover, we found augmented expression of the T<sub>H1</sub>-transcription factor Tbet and T<sub>H1</sub>-associated cytokine IFN $\gamma$  in atherosclerotic lesions of mice receiving WT but not *Csf2*<sup>-/-</sup> B cells or vehicle only (Figure 5E). However, expression of T<sub>reg</sub> transcription factor Foxp3, T<sub>reg</sub>-associated cytokines TGF $\beta$ <sub>1</sub> and IL-10, T<sub>H2</sub>-associated GATA3 and IL-4, and T<sub>H17</sub>-associated ROR $\gamma$ t and IL-17, remained unaffected (Figure 5F, G). Quantification of lesion size and morphology, as determined by ORO, Mac3, CD4, SMA, and Masson's trichrome staining, correlated these findings with those reported in Figure 2: mice receiving WT B cells had larger lesions, with more macrophages and T cells, compared to mice receiving *Csf2*<sup>-/-</sup> or no B cells (Figure 5H-L). Altogether, these data indicate that IRA B cells aggravate atherosclerosis by stimulating DC production and shifting the host response towards T<sub>H1</sub>-associated immunity (Figure 6).

## Discussion

DC are professional antigen presenting cells that, in the context of secondary signals such as IL-12, can generate IFN $\gamma$ -producing T<sub>H1</sub> cells capable of activating macrophages and promoting isotype switching in B cells. In atherosclerosis, T<sub>H1</sub>-type immunity promotes disease, but the orchestrating pathways remain poorly understood<sup>37</sup>. This study reveals that IRA B cells can shape immunity in atherosclerosis. By expressing GM-CSF in microenvironments that support the production of mature DC, IRA B cells operate in a strategic location and deliver a potent signal that instructs the host to mount an adaptive-like immune response.

In murine disease models that depend on antigen sensitization and challenge, such as rheumatoid arthritis, multiple sclerosis, and myocarditis, GM-CSF deficiency ameliorates disease<sup>38–41</sup>, suggesting a major role for the growth factor in DC-mediated generation of adaptive immunity. Our data expand on these observations by showing that, in atherosclerosis, IRA B cells are major sources of DC-promoting GM-CSF. In the steady state, when IRA B cells are exceedingly rare – or when they are absent altogether – splenic DCs develop normally, indicating that cellular sources other than IRA B cells maintain this population. In response to danger, however, mobilization of IRA B cells stimulates the developmental expansion of mature CD11b<sup>+</sup> cDC, a subset whose dependence on GM-CSF in atherosclerosis was previously unrecognized. These changes translate to the increase of IFN $\gamma$ -producing T cells and OxLDL-specific and T<sub>H1</sub>-dependent IgG2c antibodies.

Assessing the role of B cells in atherosclerosis is complex, in part due to the difficulty in separating the intrinsic biological effects of B cells from the effects of the antibodies they secrete, and because of the increasing evidence for a variety of functionally distinct B cell subsets<sup>42</sup>. Considerable data support an atheroprotective role of B1 cells, particularly B1a cells, which are believed to protect from atherosclerosis by secreting natural oxidized lipoprotein-scavenging IgM antibodies. Controversy surrounds the role of B2 cells, however, which are the main producers of adaptive IgG antibodies. Clinically, high anti-oxLDL IgG levels in cardiovascular patients positively correlate with disease burden<sup>43, 44</sup>. But how do they function? On the one hand, IgG-mediated antigen scavenging may provide protection, similar to natural IgM antibodies. On the other hand, IgG isotypes bind variably to different Fc receptors, which can either activate or inhibit target cells such as macrophages, irrespective of antigen binding. Signalling via different Fc receptors can thus have opposing effects on atherosclerosis, as studies in mice deficient either for the activating Fc $\gamma$ R or the inhibitory Fc $\gamma$ RIIb have shown<sup>42</sup>. Adding to the complexity, IgG subclasses exhibit different activation-to-inhibition ratios<sup>45</sup>. IRA B cell-dependent production of the IgG2c isotype, which has the highest ratio, may therefore be consistent with the observation that IRA B cells aggravate atherosclerosis. Beyond antibodies, B cells are also sources of cytokines and chemokines, such as regulatory IL-10<sup>6</sup> and monocyte-mobilizing MCP3/CCL7<sup>46</sup>. While the role of these subsets in atherosclerosis is still unknown, our study on yet another class of mediator – a growth factor – reveals that B cells can aggravate atherosclerosis by generating T<sub>H1</sub>-priming cDC.



One somewhat puzzling observation is that a B cell should be a major source of GM-CSF in the first place. After all, B cells participate fundamentally in humoral immunity, and so it may be counter-intuitive that B cells should also act in the generation of DC, the cells specialized in the afferent limb of the T cell response. Yet, IRA B cells may be ideally suited for a sentinel role in adaptive immunity. The spleen screens blood for pathogens and B cells are the spleen's most numerous occupants. B cells physically interact with dendritic cells in the spleen to initiate T cell-independent immunity<sup>47</sup>. Moreover, recent studies have shown that signaling via Myd88 in B cells is important to DC function in lupus and T<sub>H1</sub> priming<sup>48, 49</sup>. The finding that IRA B cells require signaling via Myd88 raises the possibility that the link between Myd88 signaling in B cells and DC function in lupus likewise involves B cell-derived GM-CSF. Strategically located and equipped with a plethora of receptors capable of recognizing molecular patterns, IRA B cells may indeed represent a cellular node that bridges innate and adaptive immunity.

The function of the pleiotropic cytokine GM-CSF depends on concentration, location, and timing of expression. Although it is remarkable that a small population of B cells secreting GM-CSF elicited a significant difference in lesion size, ORO area, and macrophage and T cell content, it should be noted that other leukocytes, including macrophages and T cells, can also produce GM-CSF<sup>21, 50</sup>. Therefore, attention to the cellular source may be critical to understanding a cytokine's pleiotropic behavior. This study focused on the interplay of GM-CSF-producing IRA B cells with DC partly because IRA B cells selectively increased in secondary lymphoid organs where DC reside. Even though we did not observe effects of IRA B cells on monocytes and neutrophilia, IRA B cells could elicit other effects on myeloid cells as disease progresses. Similarly, the absence of IRA B cells in the aorta in our setting does not preclude their accumulation and local influence in more advanced disease. Future studies will need to determine how alternative cellular sources of GM-CSF at various stages of disease influence atherosclerosis.

HMG-Co-A inhibitors (statins) have proven benefit in reducing cardiovascular events in individuals in broad categories of risk in part through direct antiinflammatory actions. Yet, despite treatment with the best available therapeutics, a considerable burden of residual events threatens individuals prone to complications of atherosclerosis. This challenge has energized efforts at targeting inflammation. Understanding the complex, redundant, and interlinked networks of innate and adaptive immunity implicated in atherogenesis is essential to the development of effective but nuanced immune-targeting approaches. An integrated, systems-wide model that charts how the immune system recognizes harmful atherosclerosis-promoting molecular patterns, how it incorporates and propagates this information, and how it ultimately impacts disease should aid the development of specific and finely-tuned treatments. The function of IRA B cells described here illuminates a previously unknown regulatory node operating in atherosclerosis, and is worthy of consideration as a candidate for therapeutic intervention.

## Supplementary Material

Refer to Web version on PubMed Central for supplementary material.

## Acknowledgments

The authors thank Michael Waring and Adam Chicoine for sorting cells (Harvard Medical School). The authors thank Eugenia Shvartz, Thibaut Quillard and Benjamin G. Chousterman for technical support. The authors thank Andrew H. Lichtman (Brigham and Women's Hospital) for a fruitful discussion.

**Funding Sources:** This work was supported in part by NIH grants 1R01HL095612 (to F.K.S.), P01 HL 088093 (to J.L.W.), R01HL080472 (to P.L.), and Canadian Institutes of Health Research grant MOP 126205 (to B.B.R.). I.H. was supported by the German Research Foundation and the Society of Thrombosis and Haemostasis Research. I.T. was supported by the Max Kade Foundation. L.M.S.G. was supported by the Boehringer Ingelheim Funds. G.F.W. was supported by the German Research Foundation. C.S.R. was supported by the American Heart Association postdoctoral fellowship and the Massachusetts General Hospital Executive Committee on Research Postdoctoral Award.

## References

1. Ait-Oufella H, Salomon BL, Potteaux S, Robertson AK, Gourdy P, Zoll J, Merval R, Esposito B, Cohen JL, Fisson S, Flavell RA, Hansson GK, Klatzmann D, Tedgui A, Mallat Z. Natural regulatory T cells control the development of atherosclerosis in mice. *Nat Med.* 2006; 12:178–180. [PubMed: 16462800]
2. Buono C, Binder CJ, Stavrakis G, Witztum JL, Glimcher LH, Lichtman AH. T-bet deficiency reduces atherosclerosis and alters plaque antigen-specific immune responses. *Proc Natl Acad Sci U S A.* 2005; 102:1596–1601. [PubMed: 15665085]
3. Herbin O, Ait-Oufella H, Yu W, Fredrikson GN, Aubier B, Perez N, Barateau V, Nilsson J, Tedgui A, Mallat Z. Regulatory T-cell response to apolipoprotein B100-derived peptides reduces the development and progression of atherosclerosis in mice. *Arterioscler Thromb Vasc Biol.* 2012; 32:605–612. [PubMed: 22223728]
4. Klingenberg R, Gerdes N, Badeau RM, Gistera A, Strodtzoff D, Ketelhuth DF, Lundberg AM, Rudling M, Nilsson SK, Olivecrona G, Zoller S, Lohmann C, Luscher TF, Jauhiainen M, Sparwasser T, Hansson GK. Depletion of FOXP3+ regulatory T cells promotes hypercholesterolemia and atherosclerosis. *J Clin Invest.* 2013; 123:1323–1334. [PubMed: 23426179]
5. Kyaw T, Tay C, Krishnamurthi S, Kanellakis P, Agrotis A, Tipping P, Bobik A, Toh BH. B1a B lymphocytes are atheroprotective by secreting natural IgM that increases IgM deposits and reduces necrotic cores in atherosclerotic lesions. *Circ Res.* 2011; 109:830–840. [PubMed: 21868694]
6. Perry HM, McNamara CA. Refining the role of B cells in atherosclerosis. *Arterioscler Thromb Vasc Biol.* 2012; 32:1548–1549. [PubMed: 22699274]
7. Subramanian M, Thorp E, Hansson GK, Tabas I. Treg-mediated suppression of atherosclerosis requires MYD88 signaling in DCs. *J Clin Invest.* 2013; 123:179–188. [PubMed: 23257360]
8. Swirski FK, Libby P, Aikawa E, Alcaide P, Luscinskas FW, Weissleder R, Pittet MJ. Ly-6Chi monocytes dominate hypercholesterolemia-associated monocytosis and give rise to macrophages in atheromata. *J Clin Invest.* 2007; 117:195–205. [PubMed: 17200719]
9. Swirski FK, Nahrendorf M. Leukocyte behavior in atherosclerosis, myocardial infarction, and heart failure. *Science.* 2013; 339:161–166. [PubMed: 23307733]
10. Whitman SC, Ravisankar P, Elam H, Daugherty A. Exogenous interferon-gamma enhances atherosclerosis in apolipoprotein E<sup>-/-</sup> mice. *Am J Pathol.* 2000; 157:1819–1824. [PubMed: 11106554]
11. Rauch PJ, Chudnovskiy A, Robbins CS, Weber GF, Eitzrodt M, Hilgendorf I, Tiglaio E, Figueiredo JL, Iwamoto Y, Theurl I, Gorbatov R, Waring MT, Chicoine AT, Mouded M, Pittet MJ, Nahrendorf M, Weissleder R, Swirski FK. Innate response activator B cells protect against microbial sepsis. *Science.* 2012; 335:597–601. [PubMed: 22245738]
12. Stanley E, Lieschke GJ, Grail D, Metcalf D, Hodgson G, Gall JA, Maher DW, Cebon J, Sinickas V, Dunn AR. Granulocyte/macrophage colony-stimulating factor-deficient mice show no major perturbation of hematopoiesis but develop a characteristic pulmonary pathology. *Proc Natl Acad Sci U S A.* 1994; 91:5592–5596. [PubMed: 8202532]

13. Hamilton JA, Achuthan A. Colony stimulating factors and myeloid cell biology in health and disease. *Trends Immunol.* 2013; 34:81–89. [PubMed: 23000011]
14. Robbins CS, Chudnovskiy A, Rauch PJ, Figueiredo JL, Iwamoto Y, Gorbatov R, Etzrodt M, Weber GF, Ueno T, van Rooijen N, Mulligan-Kehoe MJ, Libby P, Nahrendorf M, Pittet MJ, Weissleder R, Swirski FK. Extramedullary hematopoiesis generates Ly-6C(high) monocytes that infiltrate atherosclerotic lesions. *Circulation.* 2012; 125:364–374. [PubMed: 22144566]
15. Ditiatkovski M, Toh BH, Bobik A. GM-CSF deficiency reduces macrophage PPAR-gamma expression and aggravates atherosclerosis in ApoE-deficient mice. *Arterioscler Thromb Vasc Biol.* 2006; 26:2337–2344. [PubMed: 16873730]
16. Shaposhnik Z, Wang X, Weinstein M, Bennett BJ, Lusis AJ. Granulocyte macrophage colony-stimulating factor regulates dendritic cell content of atherosclerotic lesions. *Arterioscler Thromb Vasc Biol.* 2007; 27:621–627. [PubMed: 17158354]
17. Haghghat A, Weiss D, Whalin MK, Cowan DP, Taylor WR. Granulocyte colony-stimulating factor and granulocyte macrophage colony-stimulating factor exacerbate atherosclerosis in apolipoprotein E-deficient mice. *Circulation.* 2007; 115:2049–2054. [PubMed: 17404156]
18. Zhu SN, Chen M, Jongstra-Bilen J, Cybulsky MI. GM-CSF regulates intimal cell proliferation in nascent atherosclerotic lesions. *J Exp Med.* 2009; 206:2141–2149. [PubMed: 19752185]
19. Murphy AJ, Akhtari M, Tolani S, Pagler T, Bijl N, Kuo CL, Wang M, Sanson M, Abramowicz S, Welch C, Bochem AE, Kuivenhoven JA, Yvan-Charvet L, Tall AR. ApoE regulates hematopoietic stem cell proliferation, monocytoysis, and monocyte accumulation in atherosclerotic lesions in mice. *J Clin Invest.* 2011; 121:4138–4149. [PubMed: 21968112]
20. Doran AC, Lipinski MJ, Oldham SN, Garmey JC, Campbell KA, Skaflen MD, Cutchins A, Lee DJ, Glover DK, Kelly KA, Galkina EV, Ley K, Witztum JL, Tsimikas S, Bender TP, McNamara CA. B-cell aortic homing and atheroprotection depend on Id3. *Circ Res.* 2012; 110:e1–e12. [PubMed: 22034493]
21. Sugiyama S, Okada Y, Sukhova GK, Virmani R, Heinecke JW, Libby P. Macrophage myeloperoxidase regulation by granulocyte macrophage colony-stimulating factor in human atherosclerosis and implications in acute coronary syndromes. *Am J Pathol.* 2001; 158:879–891. [PubMed: 11238037]
22. Gupta S, Pablo AM, Jiang X, Wang N, Tall AR, Schindler C. IFN-gamma potentiates atherosclerosis in ApoE knock-out mice. *J Clin Invest.* 1997; 99:2752–2761. [PubMed: 9169506]
23. McLaren JE, Ramji DP. Interferon gamma: a master regulator of atherosclerosis. *Cytokine Growth Factor Rev.* 2009; 20:125–135. [PubMed: 19041276]
24. Hermansson A, Ketelhuth DF, Strodthoff D, Wurm M, Hansson EM, Nicoletti A, Paulsson-Berne G, Hansson GK. Inhibition of T cell response to native low-density lipoprotein reduces atherosclerosis. *J Exp Med.* 2010; 207:1081–1093. [PubMed: 20439543]
25. Stemme S, Faber B, Holm J, Wiklund O, Witztum JL, Hansson GK. T lymphocytes from human atherosclerotic plaques recognize oxidized low density lipoprotein. *Proc Natl Acad Sci U S A.* 1995; 92:3893–3897. [PubMed: 7732003]
26. Zhou X, Robertson AK, Hjerpe C, Hansson GK. Adoptive transfer of CD4+ T cells reactive to modified low-density lipoprotein aggravates atherosclerosis. *Arterioscler Thromb Vasc Biol.* 2006; 26:864–870. [PubMed: 16456097]
27. Binder CJ, Horkko S, Dewan A, Chang MK, Kieu EP, Goodyear CS, Shaw PX, Palinski W, Witztum JL, Silverman GJ. Pneumococcal vaccination decreases atherosclerotic lesion formation: molecular mimicry between *Streptococcus pneumoniae* and oxidized LDL. *Nat Med.* 2003; 9:736–743. [PubMed: 12740573]
28. Zhou X, Caligiuri G, Hamsten A, Lefvert AK, Hansson GK. LDL immunization induces T-cell-dependent antibody formation and protection against atherosclerosis. *Arterioscler Thromb Vasc Biol.* 2001; 21:108–114. [PubMed: 11145941]
29. Chou MY, Fogelstrand L, Hartvigsen K, Hansen LF, Woelkers D, Shaw PX, Choi J, Perkmann T, Backhed F, Miller YI, Horkko S, Corr M, Witztum JL, Binder CJ. Oxidation-specific epitopes are dominant targets of innate natural antibodies in mice and humans. *J Clin Invest.* 2009; 119:1335–1349. [PubMed: 19363291]

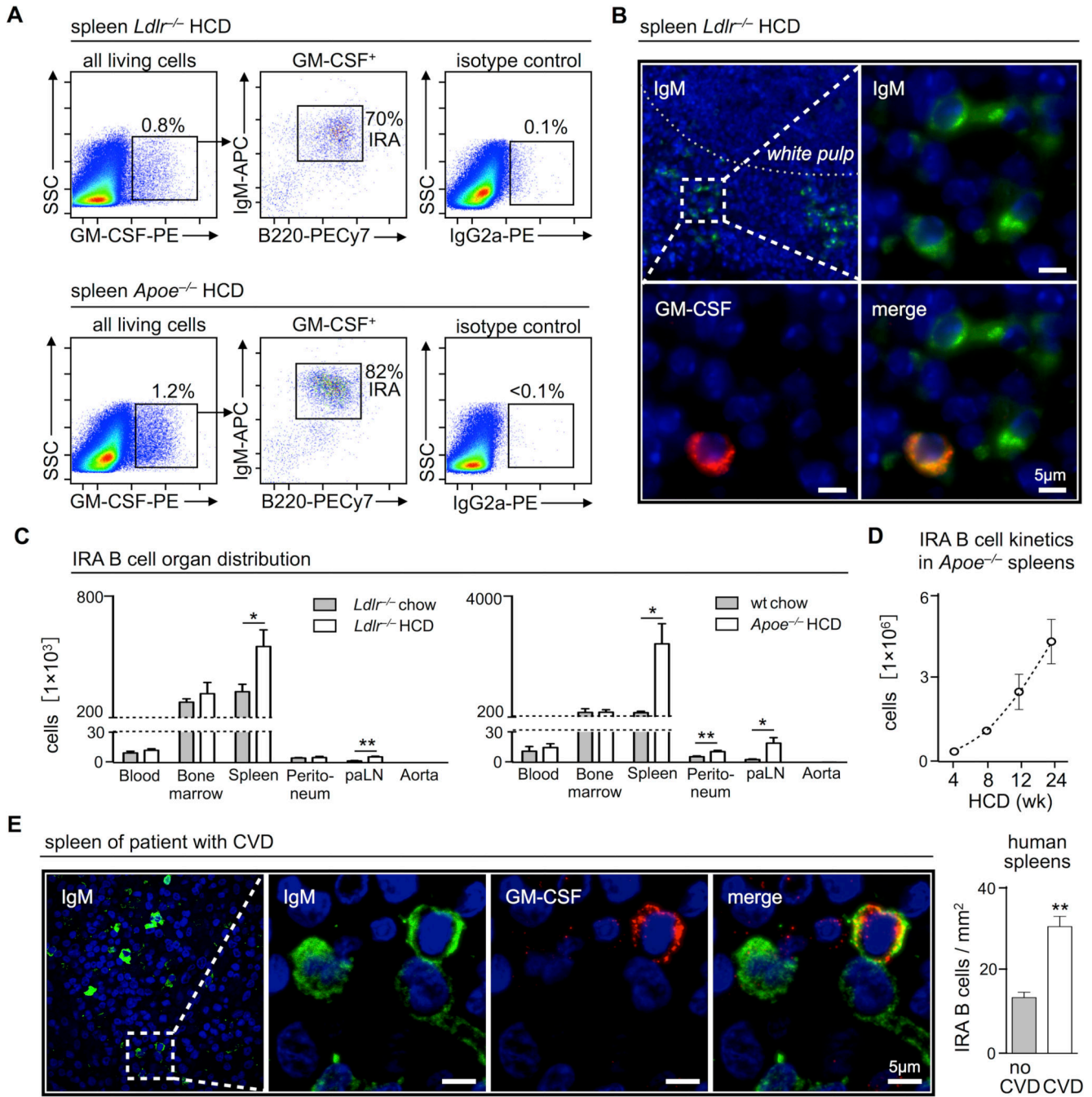
30. Stavnezer J, Amemiya CT. Evolution of isotype switching. *Semin Immunol.* 2004; 16:257–275. [PubMed: 15522624]
31. Rosas M, Gordon S, Taylor PR. Characterisation of the expression and function of the GM-CSF receptor alpha-chain in mice. *Eur J Immunol.* 2007; 37:2518–2528. [PubMed: 17694571]
32. Mallat Z, Taleb S, Ait-Oufella H, Tedgui A. The role of adaptive T cell immunity in atherosclerosis. *J Lipid Res.* 2009; 50(Suppl):S364–S369. [PubMed: 19050311]
33. Vremec D, Lieschke GJ, Dunn AR, Robb L, Metcalf D, Shortman K. The influence of granulocyte/macrophage colony-stimulating factor on dendritic cell levels in mouse lymphoid organs. *Eur J Immunol.* 1997; 27:40–44. [PubMed: 9021996]
34. Greter M, Helft J, Chow A, Hashimoto D, Mortha A, Agudo-Cantero J, Bogunovic M, Gautier EL, Miller J, Leboeuf M, Lu G, Aloman C, Brown BD, Pollard JW, Xiong H, Randolph GJ, Chipuk JE, Frenette PS, Merad M. GM-CSF controls nonlymphoid tissue dendritic cell homeostasis but is dispensable for the differentiation of inflammatory dendritic cells. *Immunity.* 2012; 36:1031–1046. [PubMed: 22749353]
35. Hamilton JA. Colony-stimulating factors in inflammation and autoimmunity. *Nat Rev Immunol.* 2008; 8:533–544. [PubMed: 18551128]
36. Daro E, Pulendran B, Brasel K, Teepe M, Pettit D, Lynch DH, Vremec D, Robb L, Shortman K, McKenna HJ, Maliszewski CR, Maraskovsky E. Polyethylene glycol-modified GM-CSF expands CD11b(high)CD11c(high) but not CD11b(low)CD11c(high) murine dendritic cells in vivo: a comparative analysis with Flt3 ligand. *J Immunol.* 2000; 165:49–58. [PubMed: 10861034]
37. Hansson GK, Hermansson A. The immune system in atherosclerosis. *Nat Immunol.* 2011; 12:204–212. [PubMed: 21321594]
38. Campbell IK, Rich MJ, Bischof RJ, Dunn AR, Grail D, Hamilton JA. Protection from collagen-induced arthritis in granulocyte-macrophage colony-stimulating factor-deficient mice. *J Immunol.* 1998; 161:3639–3644. [PubMed: 9759887]
39. McQualter JL, Darwiche R, Ewing C, Onuki M, Kay TW, Hamilton JA, Reid HH, Bernard CC. Granulocyte macrophage colony-stimulating factor: a new putative therapeutic target in multiple sclerosis. *J Exp Med.* 2001; 194:873–882. [PubMed: 11581310]
40. Sonderegger I, Iezzi G, Maier R, Schmitz N, Kurrer M, Kopf M. GM-CSF mediates autoimmunity by enhancing IL-6-dependent Th17 cell development and survival. *J Exp Med.* 2008; 205:2281–2294. [PubMed: 18779348]
41. King IL, Kroenke MA, Segal BM. GM-CSF-dependent, CD103+ dermal dendritic cells play a critical role in Th effector cell differentiation after subcutaneous immunization. *J Exp Med.* 2010; 207:953–961. [PubMed: 20421390]
42. Witztum JL, Lichtman AH. The Influence of Innate and Adaptive Immune Responses on Atherosclerosis. *Annu Rev Pathol.* 2014 Jan 24;9:73–102. Epub 2013 Aug 7. [PubMed: 23937439]
43. Ravandi A, Boekholdt SM, Mallat Z, Talmud PJ, Kastelein JJ, Wareham NJ, Miller ER, Benessiano J, Tedgui A, Witztum JL, Khaw KT, Tsimikas S. Relationship of IgG and IgM autoantibodies and immune complexes to oxidized LDL with markers of oxidation and inflammation and cardiovascular events: results from the EPIC-Norfolk Study. *J Lipid Res.* 2011; 52:1829–1836. [PubMed: 21821825]
44. Tsimikas S, Brilakis ES, Lennon RJ, Miller ER, Witztum JL, McConnell JP, Kornman KS, Berger PB. Relationship of IgG and IgM autoantibodies to oxidized low density lipoprotein with coronary artery disease and cardiovascular events. *J Lipid Res.* 2007; 48:425–433. [PubMed: 17093289]
45. Nimmerjahn F, Ravetch JV. Divergent immunoglobulin g subclass activity through selective Fc receptor binding. *Science.* 2005; 310:1510–1512. [PubMed: 16322460]
46. Zougari Y, Ait-Oufella H, Bonnin P, Simon T, Sage AP, Guerin C, Vilar J, Caligiuri G, Tsiantoulas D, Laurans L, Dumeau E, Kotti S, Bruneval P, Charo IF, Binder CJ, Danchin N, Tedgui A, Tedder TF, Silvestre JS, Mallat Z. B lymphocytes trigger monocyte mobilization and impair heart function after acute myocardial infarction. *Nat Med.* 2013; 19:1273–1280. [PubMed: 24037091]
47. Balazs M, Martin F, Zhou T, Kearney J. Blood dendritic cells interact with splenic marginal zone B cells to initiate T-independent immune responses. *Immunity.* 2002; 17:341–352. [PubMed: 12354386]

48. Teichmann LL, Schenten D, Medzhitov R, Kashgarian M, Shlomchik MJ. Signals via the adaptor MyD88 in B cells and DCs make distinct and synergistic contributions to immune activation and tissue damage in lupus. *Immunity*. 2013; 38:528–540. [PubMed: 23499488]
49. Barr TA, Brown S, Mastroeni P, Gray D. B cell intrinsic MyD88 signals drive IFN-gamma production from T cells and control switching to IgG2c. *J Immunol*. 2009; 183:1005–1012. [PubMed: 19542370]
50. Ponomarev ED, Shriver LP, Maresz K, Pedras-Vasconcelos J, Verthelyi D, Dittel BN. GM-CSF production by autoreactive T cells is required for the activation of microglial cells and the onset of experimental autoimmune encephalomyelitis. *J Immunol*. 2007; 178:39–48. [PubMed: 17182538]

### Clinical Perspective

Atherosclerosis is a lipid-driven inflammatory disease, yet treatment regimens currently lack genuinely anti-inflammatory approaches. The growth of human and mouse atherosclerotic lesions is characterized by the influx of functionally diverse leukocytes to the vessel wall. Because leukocytosis is a risk factor for complications of atherosclerosis in humans, understanding how leukocytes affect the course of disease is important, and may lead to new strategies that either augment or attenuate particular leukocyte function. This study shows that a previously unknown leukocyte population plays an important role in atherosclerosis. Innate response activator (IRA) B cells develop in lymphoid organs in humans with atherosclerosis at high numbers and in the two major mouse models. Functionally, IRA B cells aggravate atherosclerosis by shaping Th1-type adaptive immunity. The study identifies an upstream node of leukocyte communication and suggests that targeting IRA B cell function might be a strategy for the treatment of cardiovascular disease.

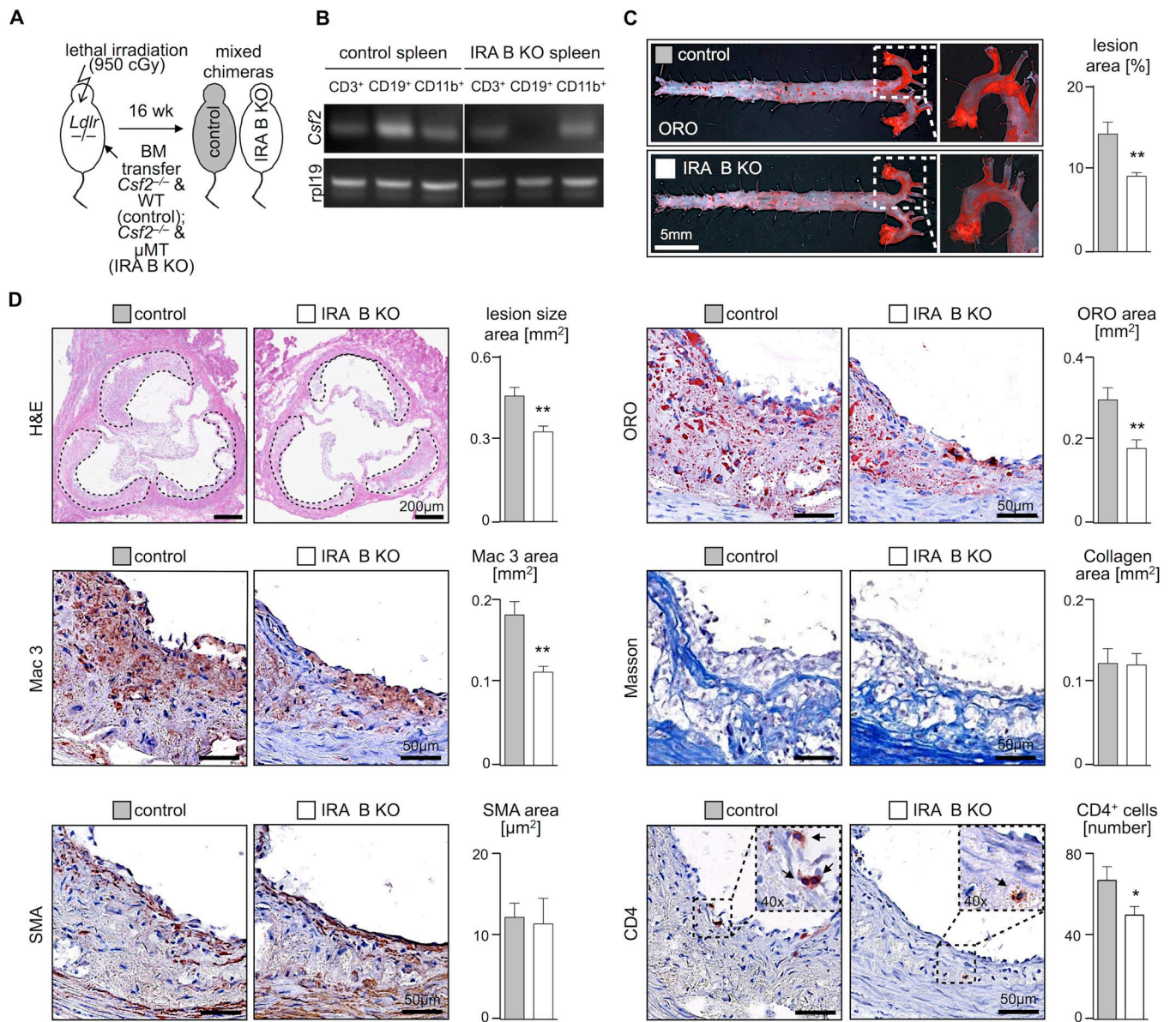




**Figure 1.**

GM-CSF producing IRA B cells expand in atherosclerosis. (A) Identification of GM-CSF<sup>+</sup> B220<sup>+</sup> IgM<sup>high</sup> IRA B cells in spleens of *Ldlr*<sup>-/-</sup> and *Apoe*<sup>-/-</sup> mice after 3 months of HCD by flow cytometry and (B) immunofluorescence histochemistry. (C) Flow cytometry based enumeration of IRA B cells in peripheral blood (per ml), total bone marrow, spleen, peritoneal lavage, four para-aortic lymph nodes and aorta in aged-matched *Ldlr*<sup>-/-</sup>, C57Bl/6 WT and *Apoe*<sup>-/-</sup> mice after 3 months of normal chow diet (gray) and HCD (white), respectively (n = 3 mice per group). Cell counts are presented as mean ± SEM, \* p < 0.05, \*\* p < 0.01, comparing chow vs. HCD per organ. (D) Kinetics of IRA B cell development in spleens of *Apoe*<sup>-/-</sup> mice. 8 week old *Apoe*<sup>-/-</sup> mice were placed on HCD and sacrificed after 4, 8, 12 and 24 weeks on HCD to quantify IRA B cell numbers (n = 3

mice per time point). Cell counts are presented as mean  $\pm$  SEM. (E) On the left, identification of IgM<sup>+</sup> GM-CSF<sup>+</sup> IRA B cells in the spleen of a patient with atherosclerosis. On the right, quantification of IRA B cells in spleen sections of patients with (white) or without (gray) symptomatic cardiovascular disease (CVD). Cells were counted in 12 randomly selected visual fields of 0.1mm<sup>2</sup> per sample. The combined number of IRA B cells in all 12 visual fields per patient was divided by the total area analyzed (12  $\times$  0.1mm<sup>2</sup>). Results are presented as means  $\pm$  SEM, \*\* p < 0.01, n = 4 per group. For all flow cytometric plots, the ticks represent 0, 10<sup>2</sup>, 10<sup>3</sup>, 10<sup>4</sup>, 10<sup>5</sup> fluorescence units, except axes labeled “SSC,” for which the ticks represent 0, 50 000, 100 000, 150 000, 200 000, and 250 000 fluorescence units.

**Figure 2.**

IRA B cells promote atherosclerosis. (A) For generation of mixed bone marrow chimeras with B cell restricted GM-CSF deficiency (IRA B KO) lethally irradiated 8 week old *Ldlr*<sup>-/-</sup> mice were reconstituted with a 50:50 mixture of GM-CSF deficient (*Csf2*<sup>-/-</sup>) and B cell deficient ( $\mu$ MT) bone marrow (white). Control mice were reconstituted with a 50:50 mixture of GM-CSF deficient (*Csf2*<sup>-/-</sup>) and WT bone marrow (gray). After 6 weeks of reconstitution mice were placed on HCD for another 10 weeks. (B) Validation of B cell restricted GM-CSF deficiency in IRA B KO mice after reconstitution and 10 weeks of HCD. Identification of GM-CSF (*Csf2*) mRNA expression by semi-quantitative reverse transcription PCR in sorted CD3<sup>+</sup> (T cells), CD19<sup>+</sup> (B cells) and CD11b<sup>+</sup> (myeloid cells) splenocytes from control and IRA B KO mice. *Rpl19* serves as the housekeeping gene. (C) En face Oil-Red-O (ORO) staining of excised aortas from control and IRA B KO mice after 10 weeks of HCD on the left and quantification of lesion area on the right (n = 7 per group). Results are presented as means  $\pm$  SEM, \*\* p 0.01, gray color for control, white color for IRA B KO mice. (D) Representative H&E staining of aortic root sections from control (gray) and IRA B KO (white) mice after 10 weeks of HCD with quantification of lesion size in two independent experiments (n = 20 per group). Results are presented as means  $\pm$  SEM. In addition immunohistology depicting ORO-, Mac3-,

smooth muscle actin (SMA)-, Masson's trichrome (Masson) and CD4-positive staining of aortic root lesions representative of both groups with quantification of n = 10 samples per group. Results are presented as mean  $\pm$  SEM, \* p < 0.05, \*\* p < 0.01.



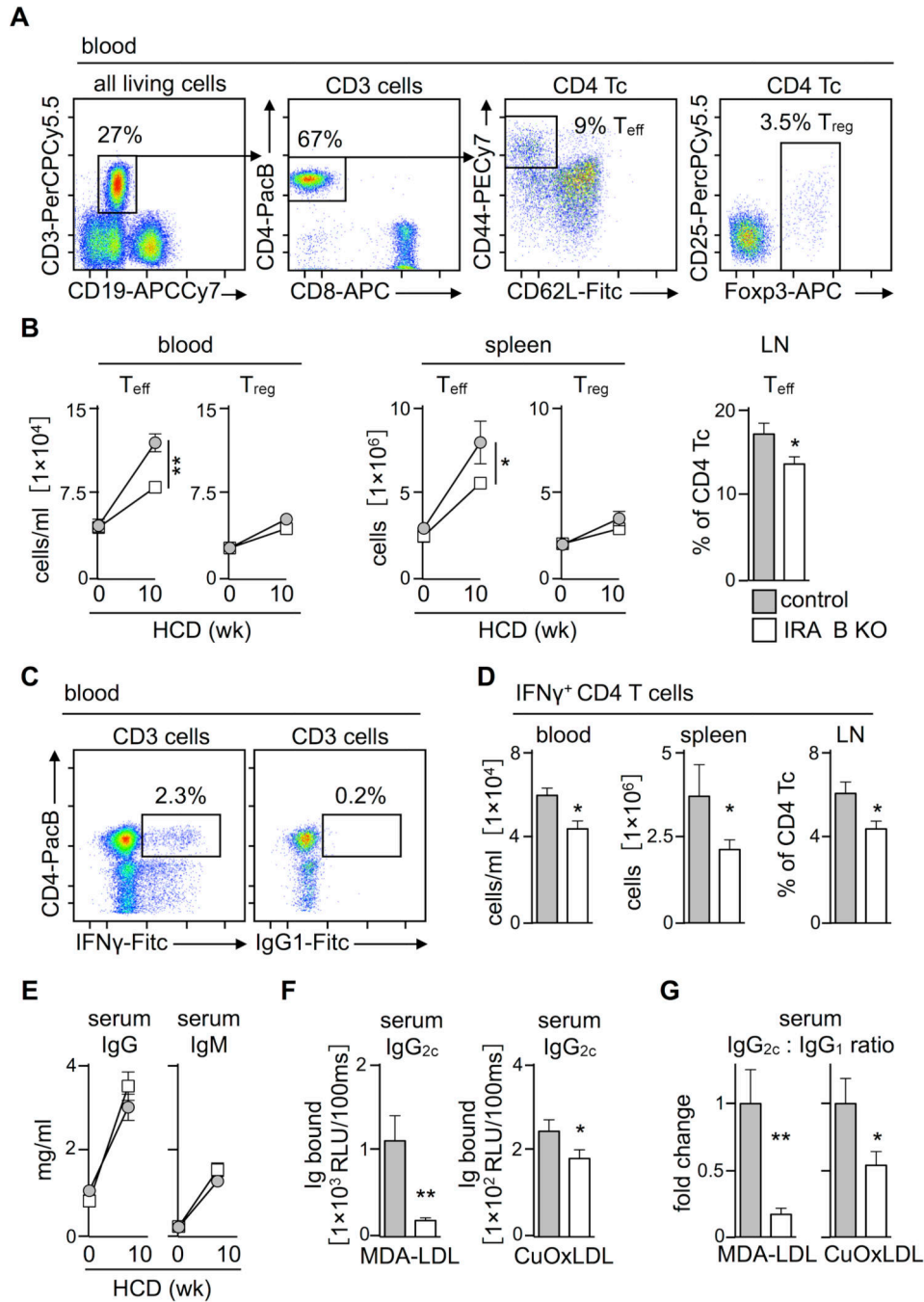


**Figure 3.**

IRA B cells promote the generation of T<sub>H1</sub> effector cells in atherosclerosis. (A) Representative dot plots showing gating for CD3<sup>+</sup> CD4<sup>+</sup> CD44<sup>high</sup> CD62L<sup>low</sup> T effector (T<sub>eff</sub>) cells and CD3<sup>+</sup> CD4<sup>+</sup> Foxp3<sup>+</sup> regulatory T cells (T<sub>reg</sub>) in blood. (B) Kinetics of T<sub>eff</sub> and T<sub>reg</sub> cell development in blood and spleen as well as proportion of T<sub>eff</sub> cells in para-aortic lymph nodes during 10 week HCD feeding of IRA B KO (white) and control (gray) mice. Results are presented as mean ± SEM, \* p < 0.05, \*\* p < 0.01, comparing IRA B KO vs. control mice at 10 weeks, n = 6 per group. (C) Representative dot plots showing gating for CD3<sup>+</sup> CD4<sup>+</sup> IFN $\gamma$ <sup>+</sup> T cells in blood. (D) Quantification of IFN $\gamma$ -producing T cells in blood, spleen and para-aortic lymph nodes after 10 week HCD feeding of IRA B KO (white) and control (gray) mice. Results are presented as mean ± SEM, \* p < 0.05, n = 10

per group. (E) Kinetics of total IgG and IgM serum levels during 10 week HCD feeding of IRA B KO (white) and control (gray) mice. Results are presented as mean  $\pm$  SEM, n = 6 per group and time point. (F) Quantification of IgG<sub>2c</sub> antibody titers against MDA-LDL and copper-oxidized LDL (CuOxLDL) in 1:25 diluted individual serum samples, n = 10 per group. Results are presented as mean  $\pm$  SEM, \* p < 0.05, \*\* p < 0.01. (G) Quantitative ratio of IgG<sub>2c</sub> and IgG<sub>1</sub> titers against MDA-LDL and copper-oxidized LDL (CuOxLDL) in 1:25 diluted individual serum samples, n = 10 per group. Results are presented as mean  $\pm$  SEM fold changes of the IgG<sub>2c</sub> : IgG<sub>1</sub> ratio to illustrate shifts in isotype switching between control and IRA B KO mice, \* p < 0.05, \*\* p < 0.01.



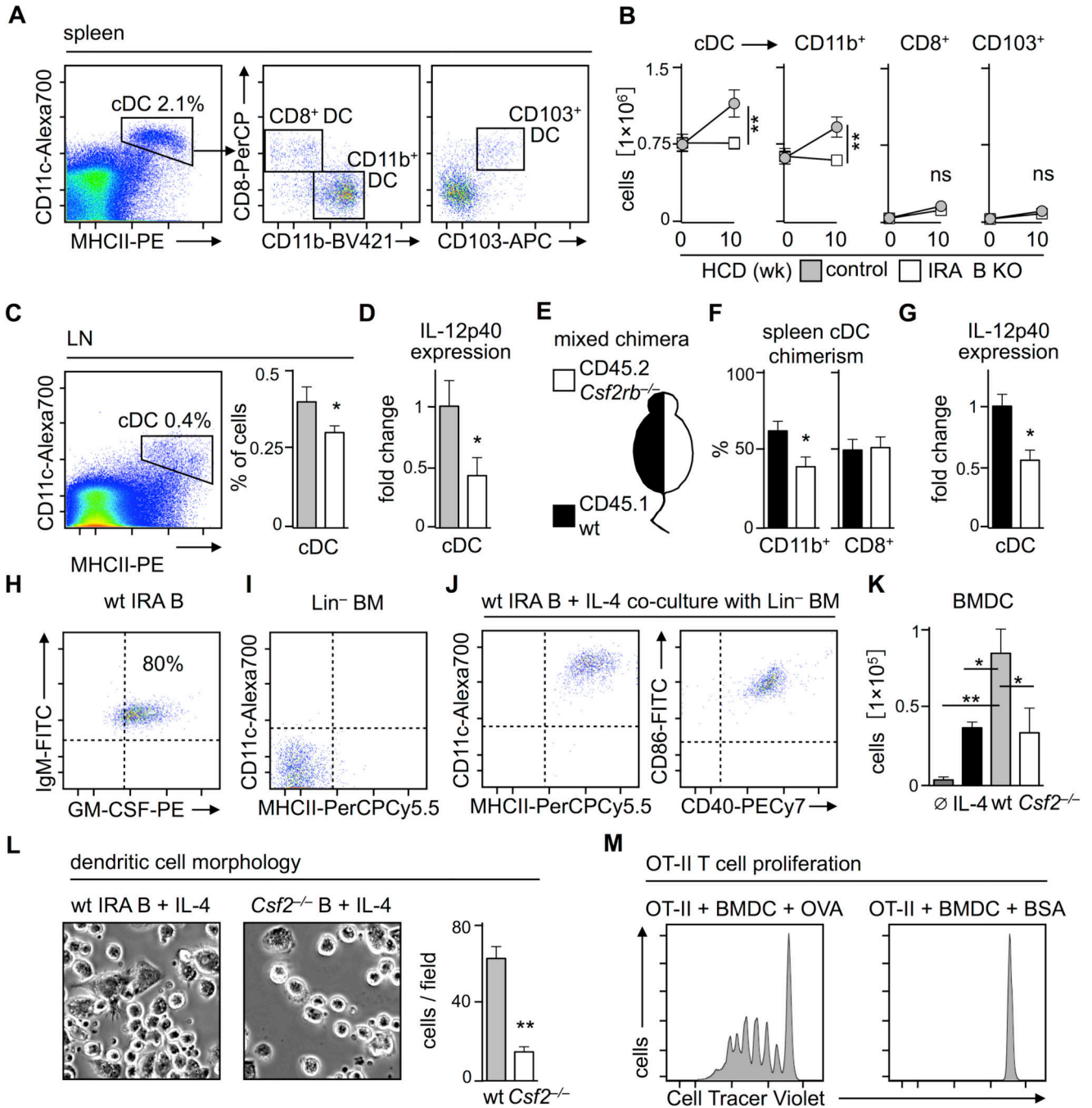


**Figure 4.**

IRA B cells promote the generation of classical dendritic cells (cDC) in atherosclerosis. (A) Representative dot plots showing gating for CD19<sup>-</sup> MHCII<sup>high</sup> CD11c<sup>high</sup> classical (c)DC, CD8<sup>-</sup> CD11b<sup>+</sup>, CD8<sup>+</sup> CD11b<sup>-</sup> and CD8<sup>+</sup> CD103<sup>+</sup> subsets in the spleen. (B) Kinetics of splenic cDC subset development during 10 week HCD feeding of IRA B KO (white) and control (gray) mice. Results are presented as mean ± SEM, \* p 0.05, \*\* p 0.01, comparing IRA B KO vs. control mice at 10 weeks, n 6 per group. (C) Identification and quantification of the proportion of cDC in para-aortic lymph nodes. Results are presented as mean ± SEM, \* p 0.05, n 10 per group. (D) Quantification of IL-12p40 expression in splenic cDC sorted from IRA B KO (white) and control (gray) mice by real-time PCR. Results are presented as mean ± SEM fold change of 2<sup>Ct</sup>, \* p 0.05, n 10

per group. (E) *Ldlr*<sup>-/-</sup> mice were lethally irradiated, reconstituted with a 50:50 mixture of CD45.1<sup>+</sup> WT (black) and CD45.2<sup>+</sup> *Csf2rb*<sup>-/-</sup> (white) bone marrow and placed on HCD for 3 months. (F) Assessment of chimerism for CD45.1 (WT in black) and CD45.2 (*Csf2rb*<sup>-/-</sup> in white) in CD11b<sup>+</sup> and CD8<sup>+</sup> splenic cDC. Results are presented as mean ± SEM, \* p < 0.05, n = 5 per group. (G) Quantification of IL-12p40 expression in sorted CD45.1 (WT in black) and CD45.2 (*Csf2rb*<sup>-/-</sup> in white) splenic cDC by real-time PCR. Results are presented as mean ± SEM fold change of 2<sup>-Ct</sup>, \* p < 0.05, n = 5 per group. (H) Flow assisted cell sorting of CD23<sup>low</sup> IgM<sup>high</sup> CD43<sup>high</sup> CD138<sup>high</sup> cells from WT and *Csf2*<sup>-/-</sup> mice after 4 × 25mg/day LPS i.p. Representative dot plot showing enrichment for GM-CSF<sup>+</sup> IRA B cells in WT mice. Dashed lines represent isotype controls. (I) Representative dot plot showing MHCII and CD11c expression in lineage depleted (Lin = CD3, CD90.2, CD19, B220, NK1.1, Ly6G) CD45.1<sup>+</sup> bone marrow cells before in vitro culture. Dashed lines represent isotype controls. (J) Representative dot plot showing high MHCII, CD11c, CD86 and CD40 expression on bone marrow derived DC (BMDC) generated through co-culture with IRA B cells and IL-4 over 8 days. Dashed lines represent isotype controls. (K) Enumeration of MHCII<sup>+</sup> CD11c<sup>+</sup> BMDC after co-culture with medium alone (dark gray), medium plus IL-4 (black), IRA B cells and IL-4 (gray), or corresponding B cells from LPS challenged GM-CSF<sup>-/-</sup> mice with IL-4 (white). Results are presented as mean ± SEM, \* p < 0.05, comparing WT vs. all other groups by ANOVA, n = 3 per group. (L) Evaluation of dendritic cell morphology of BMDC generated with IRA B cells or *Csf2*<sup>-/-</sup> B cells. Representative phase contrast microscopy images are shown on the left. Quantification of cells with typical dendritiform protrusions per visual field is shown on the right. Results are presented as mean ± SEM analyzed in 6 visual fields per well and group, \* p < 0.05, \*\* p < 0.01. (M) CD4<sup>+</sup> CD25<sup>-</sup> OT-II cells were co-cultured with IRA B cell-generated BMDC loaded with ovalbumin (OVA; 100µg/ml) or BSA (100µg/ml) for 4 days. Representative histograms show cell divisions of OT-II T cells labeled with a cell tracer dye.

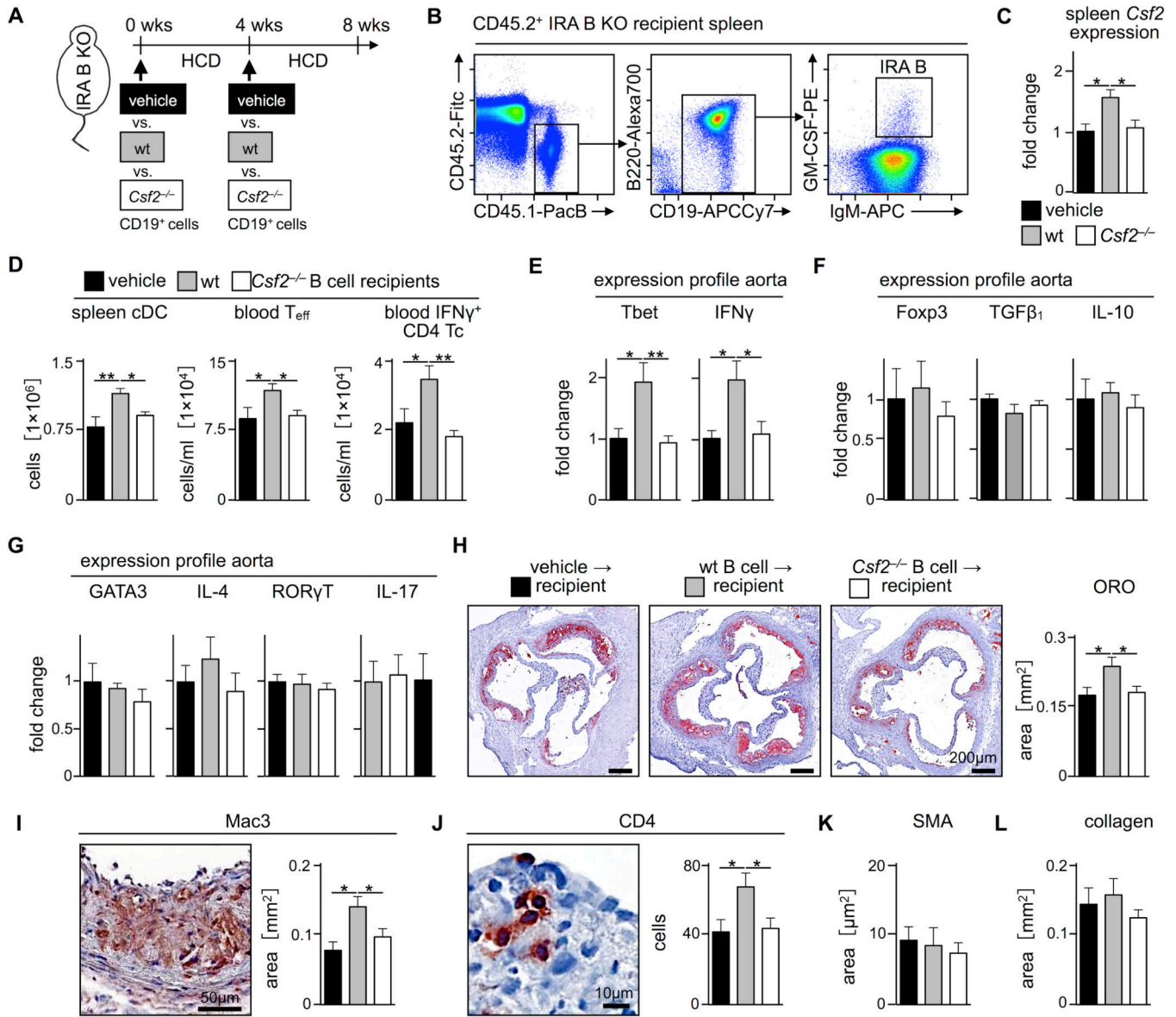


**Figure 5.**

Transfer of GM-CSF competent B cells aggravates atherosclerosis. (A) Experimental strategy for B cell adoptive transfer. Naive IRA B KO mice were divided into three groups receiving either  $2.5 \times 10^7$  CD19<sup>+</sup> B cells from WT (gray) or Csf2<sup>-/-</sup> (white) mice (n = 7 per group) or vehicle (DPBS) alone (black) (n = 5) at week 0 and 4 of a 8 week period of HCD feeding. (B) Representative dot plots showing identification of IRA B cells in the spleen of a CD45.2<sup>+</sup> IRA B KO recipient on HCD 8 weeks after transfer of  $25 \times 10^6$  CD45.1<sup>+</sup> WT B cells twice, 4 weeks apart. (C) Quantification of GM-CSF (Csf2) expression in whole spleen tissue of IRA B KO mice 8 weeks after transfer of WT (gray), Csf2<sup>-/-</sup> (white) (n = 7 per group) or no B cells (black; n = 5) by real-time PCR. Results are presented as mean  $\pm$  SEM fold change of 2<sup>Ct</sup>, \* p < 0.05, comparing WT vs. the other groups by ANOVA. (D) Enumeration of spleen cDC, blood T effector cells, and blood IFN $\gamma$ -producing T cells in recipients of WT (gray) cells compared to those receiving Csf2<sup>-/-</sup> (white) B cells (n = 7 per group) or vehicle (black; n = 5) after 8 weeks HCD feeding. Results are presented as mean  $\pm$  SEM, \* p < 0.05, comparing WT vs. the other groups by ANOVA. (E-G) Quantification of T<sub>H1</sub>-associated Tbet and IFN $\gamma$ , T<sub>reg</sub>-associated Foxp3, TGF $\beta$ <sub>1</sub> and IL-10, and T<sub>H2</sub>- and T<sub>H17</sub>-associated GATA3, IL-4, ROR $\gamma$ T and IL-17 expression in aortic tissue of WT (gray) versus Csf2<sup>-/-</sup> (white) B cell recipients (n = 7 per

group) and vehicle group (black; n = 5) by real-time PCR. Results are presented as mean  $\pm$  SEM fold change of  $2^{-Ct}$ , \* p < 0.05, comparing WT vs. the other groups by ANOVA. (H) Quantification of ORO-rich areas in aortic root sections of recipients of WT (gray) versus *Csf2<sup>-/-</sup>* (white) B cells (n = 7 per group) and vehicle group (black; n = 5) on the right and representative images on the left. Results are presented as mean  $\pm$  SEM, \* p < 0.05, comparing WT vs. the other groups by ANOVA. (I-L) Representative images and quantification of Mac3-, CD4-, SMA-positive and Masson's trichrome staining in aortic root sections of the three groups. Results are presented as mean  $\pm$  SEM, \* p < 0.05, comparing WT vs. the other groups by ANOVA.

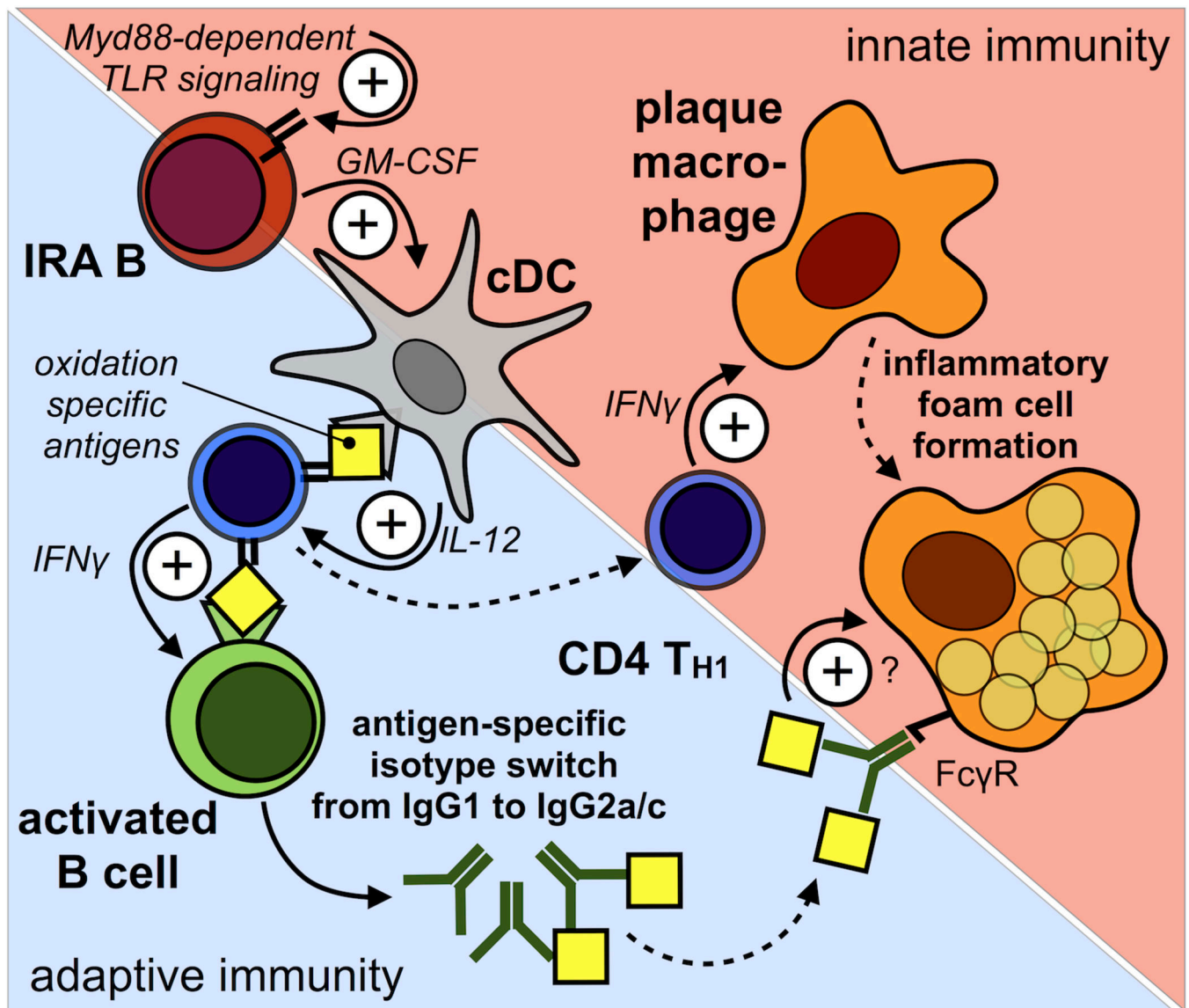


**Figure 6.**

Model of IRA B cell-dependent T<sub>H1</sub> skewing during atherosclerosis. During atherosclerosis IRA B cells arise in secondary lymphoid organs via Myd88-dependent signaling and promote the generation of classical IL-12 producing classical dendritic cells (cDC). CD4<sup>+</sup> T-helper cells that recognize disease related antigens (i.e. oxidation specific epitopes) presented by these cDC differentiate into IFN $\gamma$ -producing T<sub>H1</sub> cells. T<sub>H1</sub> cells infiltrate atherosclerotic lesions and stimulate macrophages. Antigen-specific interaction between T<sub>H1</sub> cells and B cells leads to IFN $\gamma$ -dependent isotype switching from IgG1 to IgG2a/c which carry the highest Fc $\gamma$ -receptor mediated activation capacity. By instructing T<sub>H1</sub>-priming cDC IRA B cells aid in bridging innate and adaptive immunity. Solid arrows depict functional relationship and dashed arrows depict spatial relationship.